Experimental evidence of enhanced boil-off in mobile cryogenic vessels

B Nitin[a], Pavitra Sandilya[a,*], Goutam Chakraborty[b]

[a] *Cryogenic Engineering Centre, Indian Institute of Technology Kharagpur, Kharagpur, West Bengal, 721302, India*
[b] *Department of Mechanical Engineering, Indian Institute of Technology Kharagpur, Kharagpur, West Bengal 721302, India*

Abstract

It has been postulated in the literature pertaining to the storage and transportation of cryogenic liquids that sloshing could intensify the boil-off of such liquids. However, there has been no experimental evidence in support of such postulations. Therefore, we undertook an experimental study to verify the postulation and found that the movement of the storage vessel does cause a significant increase in the boil-off. This finding will be of great help for the design engineers involved in the design and construction of storage vessels and mobile carriers. To the best of the authors' knowledge, the results of this study are the first ever proof that sloshing adds to the thermal energy over-and-above the heat inleak from the ambient, thereby causing a deterioration in the storability of the cryogenic liquids in mobile carriers. We found that the sloshing has to attain a threshold frequency before its effect on boil-off becomes significant; and above this frequency, the boil-off increases with an increase in the sloshing frequency. These findings would greatly help in bettering the design of vessels used for the storage and transport of cryogenic liquids; thus, reducing the loss of precious cryogenic liquid as well as the deleterious impact on the environment.

Keywords: Sloshing, boil-off, cryogen, storage, dewar, incipient frequency.

1. Introduction

Cryogens like liquid nitrogen (LN2), liquid hydrogen (LH2), liquid oxygen (LOX), liquid helium (LHe) and liquefied natural gas (LNG) are essential in the space [1], marine [2], energy [3], food [4], medical [5] and manufacturing [6] applications where they are used as fuel, oxidizer, refrigerant and to create inert environment. These liquids are generally stored at near atmospheric pressures in specially designed storage vessels (called dewars) to reduce the liquid boil-off. Dewars are double walled vessels with insulation in their annular space. However, due to their low boiling points and low heats of vaporization, the liquid cryogens tend to boil-off easily even under low heat inleak.

Reduction in the liquid boil-off during the storage and transportation of cryogens remains a technological challenge to date to design cryogenic storage vessels. Excessive boil-off necessitates the liquefaction of more than required amount

*Corresponding author
Email address: profsandilya@gmail.com Phone +913222283596 (Pavitra Sandilya)

of the gas; thereby causing an increase in the cost of the liquid cryogen. Furthermore, the boil-off gas (BOG) generated during the storage and transport of the liquid cryogen has to be vented out to prevent any operational hazard due to over-pressurization of the storage vessel [7, 8]. On the other hand, frequent venting of gases may have detrimental effects on the environment (in case of methane from LNG), may cause fire hazard (in case of LNG, LOX and LH2) or may lead to heath hazards like asphyxiation.

The heat inleak is usually taken to be the sole cause of liquid loss due to boil-off. Heat inleak into a stationary cryogenic storage vessel happens through two pathways, namely, insulation and the support system [9–16]. On the other hand, for a mobile cryogenic vessel, liquid sloshing is also likely to add to the BOG generation [17]. However, the effect of sloshing on liquid boil-off has not been corroborated by any experimental data. Ignoring the sloshing effect would lead the designer to over design of the dewar thus increasing its CAPEX and OPEX. Over design in the tank dimension is undesirable in applications where there is a space constraint (for example rockets).

From the above discussion, it is evident that the effects of sloshing on the boil off (besides the mechanical stability) should be taken up to reduce the over design and thus make the cryogen storage and transportation more economical. The objective of the current paper is to develop an experimental setup to demonstrate the effect of liquid sloshing on cryogen boil-off. The boil-off study under sloshing was carried out in this novel experimental setup with LN2 at atmospheric pressure. To achieve this objective, we experimentally studied the boil-off characteristics in a cryogenic storage tank on which an oscillatory motion was imposed to simulate the liquid sloshing. The study was carried out in a novel experimental setup developed by us. To the best of the authors' knowledge, this is the first study to evaluate the effects of sloshing on cryogen boil-off.

A schematic showing the various pathways of heat addition to the cryogen are as shown in Fig. 1.

2. State of the art

Liquid sloshing has been extensively studied [18–20] in relation to design of bridge piers [21], dam walls [22], sea embankments [23], water containments [24], marine vessels [25], cryogenic space vehicles [26] etc. Sloshing has been found to reduce the life of structures [27] or cause instabilities to the motion of transport vehicles [28]. On the other hand, sloshing has been used to our advantage in the form of tuned liquid dampers (TLDs) that enable high-rise buildings to withstand collapse during a seismic event [29]. Reported studies on sloshing dealt with free surface profiles of slosh waves and pressure distribution on the solid bodies (for example, [30–34]), wave breaking phenomenon [35] and sloshing induced instability of liquid carriage [36].

Popov et al. [37] suggested to model sloshing at least as a two dimensional phenomenon due to the axial displacement of the liquid free-surface under the lateral force caused by sloshing. While 2-D approach works well for rectangular

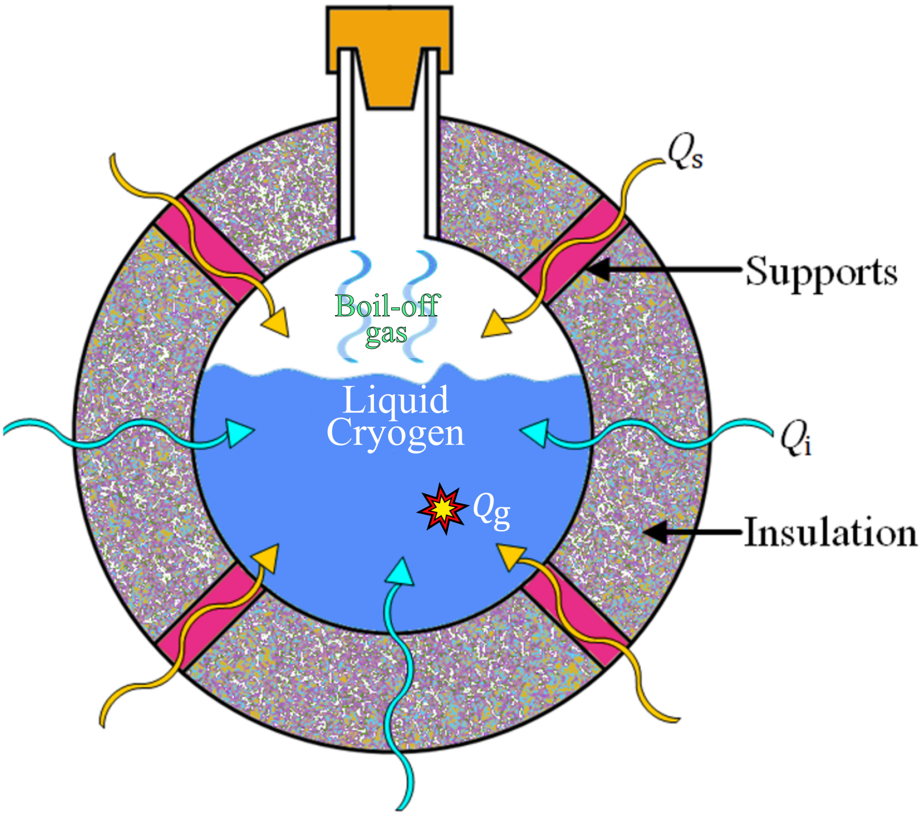

Figure 1: Various pathways of heat addition into a cryogenic storage vessel

and square tanks [38]. A 3-D approach is needed for other geometric shapes of containers like the cylindrical [39] or spherical containers [40]. Both 2-D and 3-D models models can be solved analytically under potential flow assumption [36]. Three dimensional models of sloshing generated by violent excitations have been solved using CFD techniques [41–43].

In the cryogenic applications, sloshing is observed in the storage and transportation of cryogenic liquids (LN2, LH2, LOX and LNG), in space vehicles, marine vessels and road transport. Sloshing of propellants was found to cause failure of Jupiter missiles launched by NASA [28, 44]. The failure was reportedly caused by the instability of the space vehicles due to propellant sloshing. This prompted sloshing studies in storage tanks of cryogenic propellants. Abramson [20] investigated the interactions between the orbital motion, the tank deformation and the propellant sloshing in rockets.

The hydrodynamic models developed earlier apply to the cryogenic liquid storage. In addition to these models, thermal models are also needed to understand the sloshing effects on the unique features found in cryogenic liquid dewars like stratification [45], ullage collapse [46] and easy boil-off. It has been also stated without proof that sloshing increases

Nomenclature

α	ADC count	R	Computed result
λ	Amplitude of carriage motion	s	Distance of the carriage from the ultrasonic sensor, (mm)
ρ	Liquid density, (kg/m^3)	t	time, (s)
D	Diameter of the test vessel, (m)	x	Displacement of the carriage, (mm)
f	Frequency of carriage motion, (Hz)	X_i	Measured variable i
f_c	Natural frequency of liquid column, (Hz)	ADC	Analog to Digital Converter
f_i	Incipient frequency, (Hz)	COM	Communication
g	Acceleration due to gravity, (m/s^2)	DC	Direct Current
h	Fill level of cryogen in the test vessel, (m)	FFT	Fast Fourier Transform
h	Mean liquid level, (mm)	LN2	Liquid Nitrogen
m_0	Initial mass of the tank (including its content), (kg)	LOX	Liquid Oxygen
m_t	Mass of the tank (including its content) at time t, (kg)	MOSFET	Metal Oxide Semiconductor Field Effect Transistor
$m_{\mathrm{bo},t}$	Cummulative cryogen boil-off till time t, (kg)	PC	Personal Computer
Q_g	Heat generation rate due to sloshing, (W)	PWM	Pulse Width Modulation
Q_i	Heat inleak rate through the insulation, (W)	SMPS	Switching Mode Power Supply
Q_s	Heat inleak rate through the support system, (W)	UART	Universal Asynchronous Receiver Transmitter

the cryogenic liquid boil-off [17].

Sloshing studies on cryogenic liquids are related to the study of ullage collapse and stratification. Ludwig et al. [47] studied these phenomenon by measuring the ullage pressure and liquid temperatures during sloshing. Moran et al. [48] studied the effects of slosh frequency and amplitude, pressurant type, pressure ramping, and ullage volume on the ullage pressure, and liquid and tank wall temperatures. Konopka et al. [49] studied the effects of cryogen filling and draining, and stratification on sloshing behaviour. Kim et al. [50] determined the forces on the walls of a spherical propellant tank under microgravity experimentally to validate the CFD model proposed by them to predict the pressure distribution on the container walls. Snyder [51] studied the effects of low gravity on the sloshing characteristics of liquid cryogens. Liu et al. [52, 53] investigated the effects of initial liquid fill level on the sloshing characteristics of cryogenic propellants. Grotle and Æsøy [54] studied the enhanced ullage condensation due to cryogen sloshing observed in a marine LNG tank. Xue and Lin [55] Studied the damping of liquid sloshing by using ring baffles. Liu and Lin [56] proposed a model based on spatially averaged Navier–Stokes equations to simulate non-linear and turbulent sloshing with broken free surfaces in a rectangular tank under arbitrary excitations. All these studies considered isothermal sloshing. Liu et al. [57], Grotle et al. [58], Agui and Moder [59] conducted sloshing studies under non isothermal conditions. Both the isothermal and non isothermal models were validated with experimental data using water as the working fluid. The findings from water-based sloshing studies have been applied to study the sloshing effect on the thermal stratification and ullage collapse in sloshing of cryogenic liquids (LH2 [60], LOX [61] and LNG [62–65])using the similarity principles by considering Reynold and Froude numbers. Recently, Wu and Ju [66] reported a numerical study to determine the BOG generation rate in an LNG tank under sloshing. The numerical results were validated using the experimental data on water boil-off by external electrical heating under sloshing conditions [54].

From the above discussion, it is evident that there is no experimental evidence of the significance of sloshing on the boil-off behaviour of cryogenic liquids during their mobile storage and transportation. This fact motivated us to design and develop an experimental setup that would help to study the effect of sloshing on liquid boil-off using a cryogenic liquid.

3. Design considerations

In this section we present the design considerations made to develop the experimental setup. These include the motion of the liquid container, the natural frequency of the liquid column inside the container, the limiting frequency to avoid jet formation (liquid jets are formed when liquid streams break away from the liquid mass), cumulative mass boil-off and fill level of the liquid in the container. When the imposed frequency of oscillation on the container equals the natural frequency of the liquid column inside the container, resonance occurs.

The design of the experimental setup is based on the sloshing caused by a simple harmonic motion (SHM) of a liquid container open to atmosphere. The temporal displacement of the container is given by Eq. (1).

$$x = \lambda \sin(2\pi f t) \tag{1}$$

The pressure force on the container wall generated by sloshing may damage the container. This force increases with an increase in the oscillation frequency and is maximum at the resonance condition [67]. Therefore, to avoid resonance induced damage during the carriage motion, excitation frequencies were kept less than the natural frequency of the liquid column, which is given by Eq. (2)[68].

$$f_c = \frac{1}{2\pi}\sqrt{\frac{3.68g\tanh\left(3.68\frac{h}{D}\right)}{D}} \tag{2}$$

Further, [54] showed that liquid jets formed when the frequency of oscillation was at least 84% of the natural frequency (Eq. 2). Jet formation causes violent sloshing and imparts large forces on the container walls that could damage the vessel walls. Also, since we kept the container open to the ambient, violent sloshing could cause splashing of cryogen from the vessel; and will not provide the actual boil-off rate. Therefore, we kept the oscillation frequencies below the minimum jet formation frequency. Hence, we worked with the frequencies so that Eq. (3) was satisfied.

$$f \leqslant 0.84 f_c \tag{3}$$

The cumulative boil-off up to a certain time t was determined by subtracting the mass of the vessel at time t from the initial mass of the vessel, as given by Eq. (4).

$$m_{\mathrm{bo,t}} = m_0 - m_t \tag{4}$$

The mean liquid level in the vessel at any time instant t was determined by Eq. (5).

$$h = \frac{m_t}{\frac{\pi D^2}{4}\rho} \tag{5}$$

4. Experimental

We used LN2 as the working fluid to study the sloshing effect on cryogen boil-off. LN2 was held in an insulated container, and the boil-off was determined with and without sloshing. The boil-off rates for these two cases were compared to understand would give us the effects of sloshing on cryogen boil-off.

4.1. Sloshing setup

Now, we describe the experimental setup to study the effect of sloshing on cryogen boil-off. Figure 2 shows the schematic diagram of the experimental setup.

Liquid nitrogen was held in a test vessel (1), which was held in place by putting it inside an enclosure (2). The vessel-enclosure assembly was fastened using a set of wire ropes (3) to a carriage (4) with wheels (5). Liquid sloshing was created by imparting a reciprocating motion to the carriage, which made a to-and-fro motion on a set of bounded rails(6). A load cell (7) was sandwiched between the enclosure and the carriage. The load cell measured the total weight of the test vessel and its content. A motor (8) - crank (9) - connecting rod (10) arrangement was used to impart a desired reciprocating motion to the carriage. A linear scale (11) was fixed to the rail and an ultrasonic sensor (12)

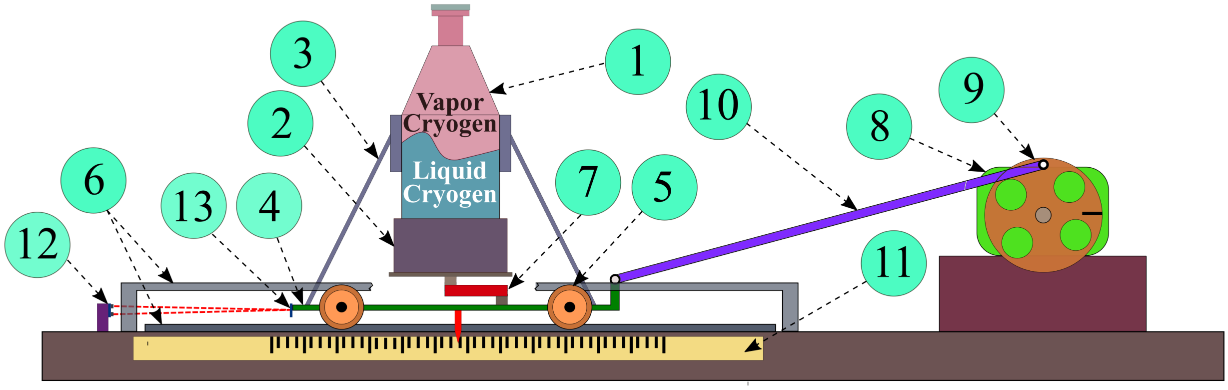

Figure 2: Schematic diagram of the experimental setup. (1) Test vessel; (2) Enclosure; (3) Wire ropes; (4) Carriage; (5) Wheels; (6) Bounded rails; (7) Load cell; (8) Motor; (9) Crank; (10) Connecting rod; (11) Linear scale; (12) Ultrasonic sensor; (13) Reflecting plate

were used to measure the amplitude and frequency of the carriage motion respectively. We developed an inhouse motor controller (described below) to vary the frequency of the carriage oscillation.

We used Arduino Uno boards to log the data from load cell and ultrasonic sensor. The Arduino Uno boards were connected to a PC via a serial COM port. We employed the UART protocol to transfer data to the PC.

Video V1 shows the CAD animation of the experimental setup and video V2 shows the working of the experimental setup.

4.2. Frequency control of carriage oscillation

A motor controller was developed in-house to regulate the motor speed. It worked on the principle of regulating the motor speed by controlling the input voltage to the motor. Figure 3 shows the architecture of the motor controller. Voltage variation across the motor (M) was achieved by the principle of pulse width modulation (PWM) [69]. Pulses were generated by ICs (IC1 and IC2); the width of the pulses was determined by manually varying the position of the potentiometer wiper controlled by the operator. In our case the rated voltage of the motor (24 V) was greater than the pulse voltage (5 V). So a push-pull amplifier made of two transistors (Q1 and Q2), was used to amplify the pulses. The amplified pulses were used to switch the state of the MOSFET (S) thereby providing a PWM input to the motor. To protect the circuit against any voltage spikes, we used a Schottky rectifier diode (D) in reverse polarity parallel to the motor as the flyback diode. The voltage required by the ICs were supplied from the mains using a regulator IC (IC3). An emergency kill switch was used to stop the carriage instantaneously while cuting off the electric supply to the setup in case of emergency.

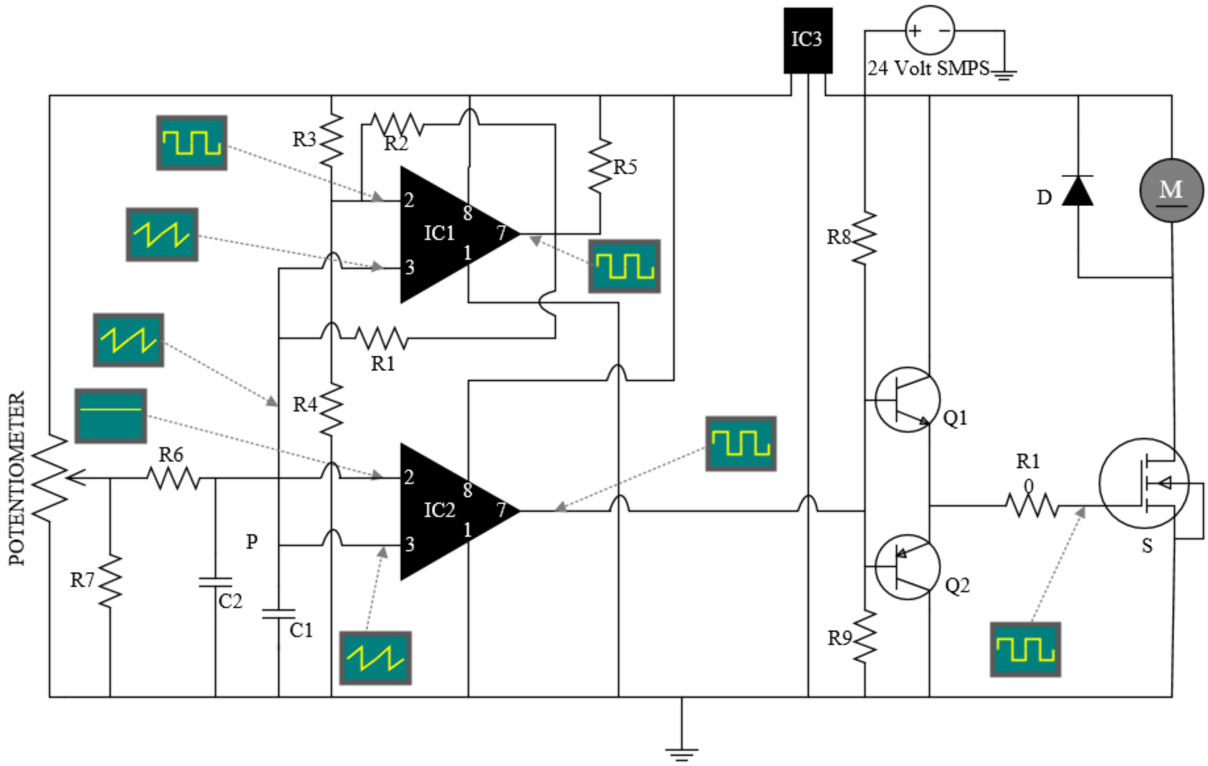

Figure 3: Architecture of the motor controller; IC1-IC3: ICs; M: Motor; S: MOSFET; Q1 and Q2: Transistors; D: Schottky diode; C1 and C2: Capacitors; R1-R10: Resistors; The waveform representation of the signals at corresponding locations is shown in green boxes.

4.3. Measurement of weight of the test vessel and its content

We used a strain gauge type load cell of 40 kg capacity (Standard Loadcells make, Model No. CZL 601 GreenLable Load cell) to measure the weight of the test vessel and its content. The output of the load cell was 2mV/V of excitation voltage. This load cell can work with 5-12 V DC. Therefore, to maximize the accuracy, we used 12 V DC from an SMPS to excite the load cell. To measure the voltage from the load cell, we developed an electronic voltage meter using an ATmega328P microcontroller-based Arduino Uno board [70] along with an external ADC module of 16 bits (ADS1115). We used the minimum voltage available with the Arduino Uno board (3.3 V DC) as reference voltage for the ADS1115 module.

4.3.1. Calibration of the load cell

We calibrated the load cell using standard weights before performing the experiments. The calibration chart is given in Fig. 4.

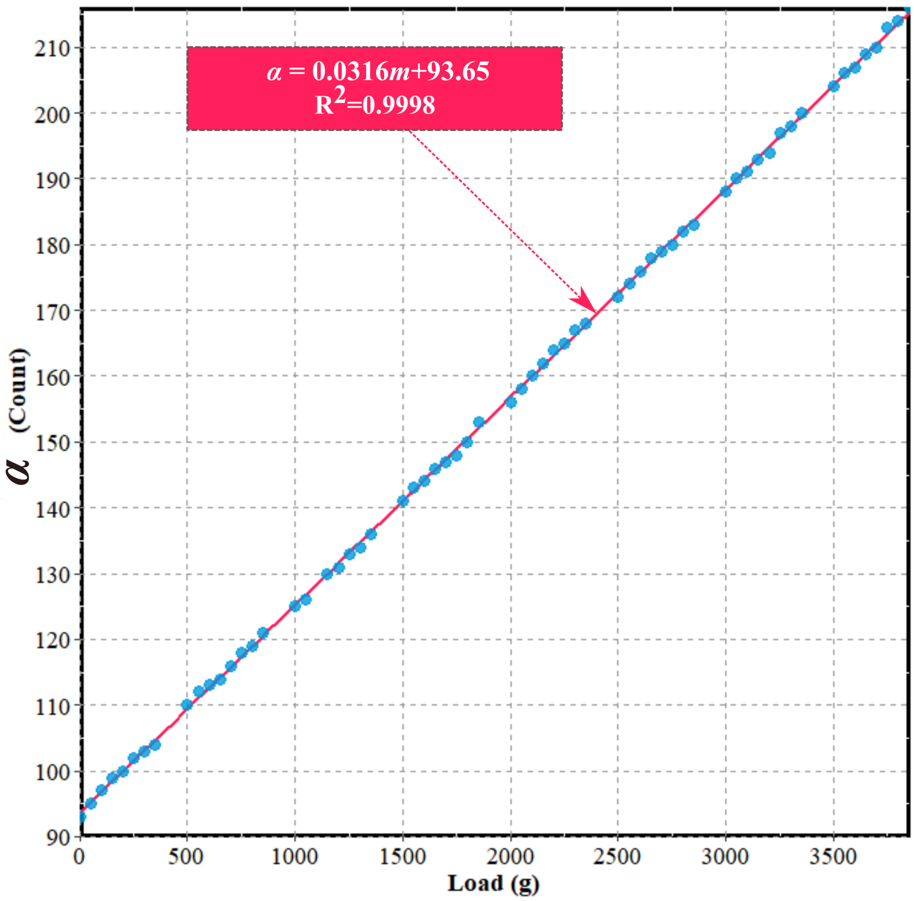

Figure 4: Calibration chart of the load cell used in the experiment

Figure 4 shows that the voltage drop in the load cell as measured by the microcontroller in ADC varies linearly with the weight as given by Eq. (6).

$$\alpha = 0.0316m + 93.65 \tag{6}$$

The load cell output usually fluctuates due to the vibrations experienced by the load cell due to the carriage motion [71]. We employed a low pass filter to filter such noise out during experimentation. The cut off frequency of the filter was found by converting the time domain data into the frequency domain using fast Fourier transform (FFT).

4.4. *Measurement of oscillation frequency*

We used an ultrasonic distance sensor module (HC-SR04) along with a reflector surface to measure the displacement of the carriage. The reflecting surface was attached to the carriage in such a manner that it was in direct view of the sensor module. The sensor module was operated with 5 V excitation voltage supplied by an Arduino Uno board.

The oscillation frequency is calculated using Eq. (7).

$$f = \frac{s}{2t\lambda} \tag{7}$$

4.5. Test vessel

We used a 10-litre vessel with foam insulation (thermal conductivity = 33 mW/m-K [72]), as the test vessel. The lateral-sectional view of the test vessel is shown in Fig. 5.

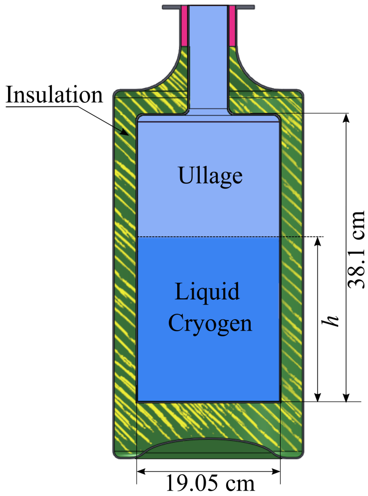

Figure 5: Lateral-sectional view of the test vessel showing the vessel dimensions; h is the height of undisturbed liquid cryogen

5. Suggested safety guidelines

While performing the experiments it is important to follow certain safety measures to protect ourselves from any hazards due to handling of cryogenic fluids and moving parts. Some relevant safety issues are given in Table 1.

Table 1: A few safety issues and their suggested preventative measures

S.No.	Possible safety issues	Suggested preventative measures
1.	Spillage of cryogenic liquids while filling up the storage vessel or during the carriage motion	•Seat the test vessel in an appropriate jig on the top platform •Fasten the vessel to the carriage, for example, by wire ropes or cables.
2.	Uncontrolled carriage motion due to failure of motor controller	•Use normally open type MOSFET as the switch (S) in the motor driver. •Mount all the heat generating components of the motor controller circuit on appropriate active or passive heat sinks.
3.	Detachment of connecting rod fixture at carriage end during operation	•Stay away from the setup while carriage is in motion.
4.	Motor drawing high current due to jamming of the wheels or overloading of the carriage	•Lubricate the rails and wheels. •Ensure that the weight of the filled vessel is below the rated load of the motor. •Monitor the current drawn by the motor. •Stop the motor if the current drawn by the motor reaches the user-defined threshold value (for example, 80% of the rated current of the motor, that is, 16 A in the proposed setup). •Use an appropriate circuit breaker in series with the motor.
5.	Seepage of condensed water vapor from the ambient into the load cell	•Make the vessel-enclosure leakproof •Make sure that there is no water in the top platform after each run of the experiment. •Ensure that the setup is in dry environment

6. Uncertainty Analysis

We used the Kline-McKlintock method [73] to estimate the uncertainties in experimental estimations. This method estimates the uncertainty in a computed result (R) using a root-sum square of the effects of each of the individual measured variables (X_i). [73]. This is given mathematically by Eq. (8).

$$\delta R = \sqrt{\sum \left(\frac{\partial R}{\partial X_i} \delta X_i \right)^2} \tag{8}$$

The uncertainties and nominal values of various measured quantities are tabulated in Table 2.

Table 2: Uncertainties and nominal values of various measurements

Quantity	Symbol (X_i)	Instrument	Uncertainty(δX_i)
ADC	α	Load cell	±1
Displacement	s	HC-SR04	±3 mm
Time	t	Arduino	±9μs
Amplitude of oscillation	λ	Linear scale	±1 mm
Diameter of the vessel	D	Linear scale	±1 mm

In our study, the uncertainty is associated with the estimation of: Cumulative boil-off, frequency of oscillation and mean liquid fill level. The determination of these uncertainties is given below.

6.1. Cumulative boil-off

The uncertainty in the estimation of cumulative boil-off ($\delta m_{\text{bo,t}}$) is a result of the measurement uncertainties of the tank mass. In this study, the uncertainty in ADC measurement (= 1 in our setup) dictates that in the tank mass. Equation (9) gives the value of $\delta m_{\text{bo,t}}$ (Eq. (8)).

Since the measured tank mass varies linearly with ADC Eq. (6), the sensitivity of the boil-off to the ADC remains the same for all the ADC values.

$$\delta m_{\text{bo,t}} = \sqrt{\left(\frac{\partial m_0}{\partial \alpha}\delta\alpha\right)^2 + \left(\frac{\partial m_t}{\partial \alpha}\delta\alpha\right)^2} \tag{9}$$

6.2. Frequency of oscillation

The sensitivities of the oscillation frequency to s, t and λ are given below,

$$\frac{\partial f}{\partial s} = \frac{1}{2\lambda t}$$
$$\frac{\partial f}{\partial t} = \frac{-s}{2\lambda t^2}$$
$$\frac{\partial f}{\partial \lambda} = \frac{-s}{2\lambda^2 t}$$

Thus we see that the sensitivity of oscillation frequency is different for different sets of s, t and λ. Applying Eq. (8) we obtain the resultant uncertainty in oscillation frequency estimation as

$$\delta f = \sqrt{\left(\frac{1}{2\lambda t}\delta s\right)^2 + \left(\frac{-s}{2\lambda t^2}\delta t\right)^2 + \left(\frac{-s}{2\lambda^2 t}\delta\lambda\right)^2} \tag{10}$$

6.3. *Mean liquid level*

The sensitivities of the mean liquid level to m_t and D are given below,

$$\frac{\partial h}{\partial \alpha} = \frac{126.58}{\pi D^2 \rho}$$
$$\frac{\partial h}{\partial D} = -\frac{253.16\alpha + 23708.8}{\pi D^3 \rho}$$

Since the measured tank mass varies linearly with ADC Eq. (6), the sensitivity of the boil-off to the ADC remains the same for all the ADC values.

Applying Eq. (8) we obtain the resultant uncertainty in mean liquid level as

$$\delta h = \sqrt{\left(\frac{126.58}{\pi D^2 \rho}\delta\alpha\right)^2 + \left(-\frac{253.16\alpha + 23708.8}{\pi D^3 \rho}\delta D\right)^2} \tag{11}$$

The uncertainties associated with the said estimations are tabulated in Table 3.

Table 3: Uncertainties in various results

Quantity	Symbol	Uncertainty
Cumulative boil-off	$m_{\text{boil-off}}$	±44.75 g
Oscillation frequency	f	±0.015 Hz
Mean liquid level	h	±1.93 mm

7. Results and Discussion

We now present the experimental results on the boil-off measurements in the test vessel at static and under dynamic conditions. The ambient temperature varied by about 1°C during an experimental run. We took an initial mass of 8 kg LN2 for all the runs. The vessels were open to the atmosphere and hence the pressure on the liquid was atmospheric (0.99 atm at 61 m altitude). To study the effects of sloshing, we first determined the natural frequency of the liquid column from Eq. (2) corresponding to the minimum estimated mean liquid level in the test vessel. This was done to ensure that the frequency of oscillation chosen to conduct the experiemnts never led to resonance. Since, the minimum fill level to cause sloshing in a container is 10% [74], we determined the natural frequency at this fill level as 1.73 Hz. As discussed earlier, we choose the maximum operable frequency as $0.84 \times 1.73 \approx 1.4$ Hz (from Eq. (3)) to avoid jet formation. Hence, the experiments were conducted with oscillation frequencies of 0.8 Hz, 1 Hz and 1.1 Hz. For our experimental setup, the amplitude of carriage oscillation was 50 mm. With the above specifications, we conducted the experiments that included noting the vessel weight with time for each frequency of oscillation.

Considerable fluctuations in the load cell signal were observed. To understand the boil-off characteristics under a given set of operating condition, we applied a low pass FFT filter to remove the high frequency noise from the signal. The frequency spectrum of the signal was considered in specifying the cut-off frequency, which should be less than the dominant noise frequency in the signal. Uniform filtering was applied for all the experimental runs by setting the cut-off frequency less than the dominant noise frequency for the 1 Hz oscillation frequency (nearly the arithmetic mean of the oscillation frequencies).

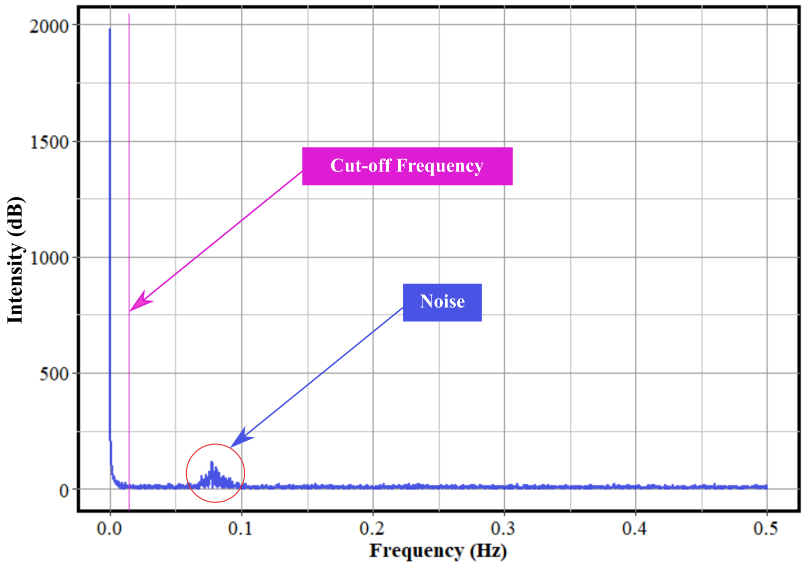

Figure 6: FFT plot of the signal from the load cell showing the noise and the selected cut-off frequency for the low pass filter

The frequency spectrum for 1 Hz oscillation case, as shown in Fig. 6, is obtained by plotting the signal intensity with the signal frequency. It is found from this figure that the signal intensity is relatively high above 0.05 Hz. We therefore chose the cut-off frequency as 0.01 Hz which is less than and away from the dominant noise frequency. The variation in the cumulative boil-off with time was determined using Eq. (4); this is shown in Fig. 7. This figure shows the un-filtered and filtered signals from the load cell. It is seen from the figure that the rate of boil-off decreases with time. Figure 8 shows the variations in the boil-off rate and the level of the liquid with time. It is seen that the boil-off rate decreased with time. This is because sloshing intensity reduces with the fall of the liquid level. A reduction in the sloshing intensity is likely to attenuate the kinetic energy of the slosh waves and hence a reduction in the boil-off [17].

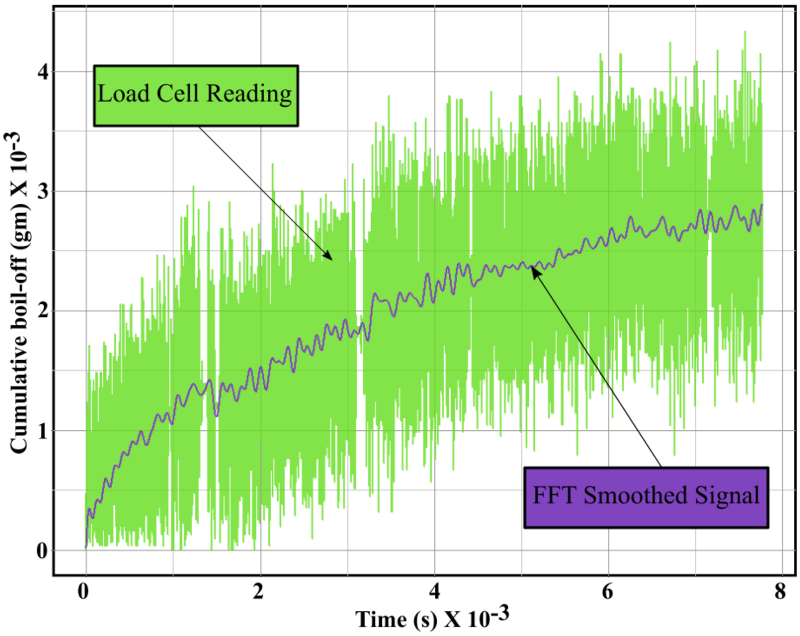

Figure 7: Load cell reading and FFT smoothed signal

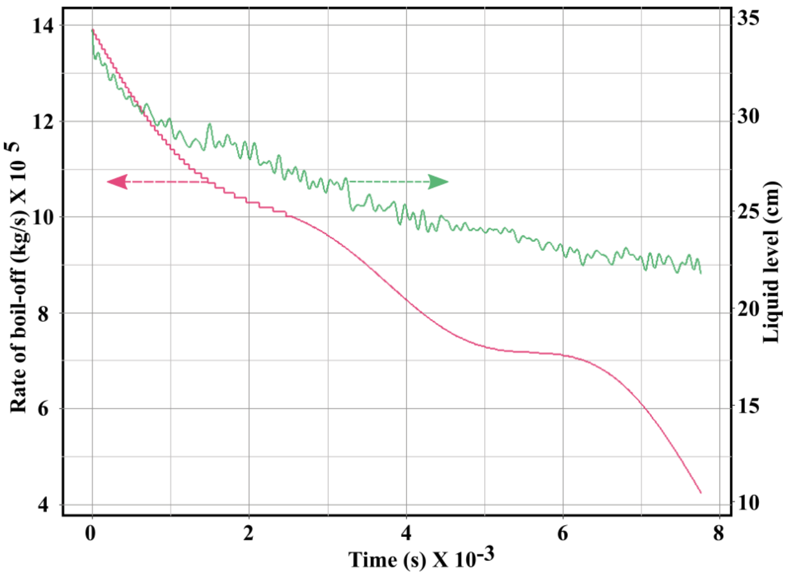

Figure 8: Rate of boil-off (red curve) and the corresponding level of liquid cryogen in the test vessel (green curve)

Figure 9 compares the boil-off history of LN2 in the test vessel for the stationary test vessel with that in each of the three oscillation frequencies employed in this study. This figure clearly demonstrates that a direct correlation exists between the sloshing frequency and the liquid boil-off. The boil-off increases with an increase in the oscillation frequency. On analysing Fig. 9 it was found that the liquid boil-off increased by 30%, 62% and 93% at oscillation frequencies of 0.8 Hz, 1 Hz and 1.1 Hz above that in the stationary case.

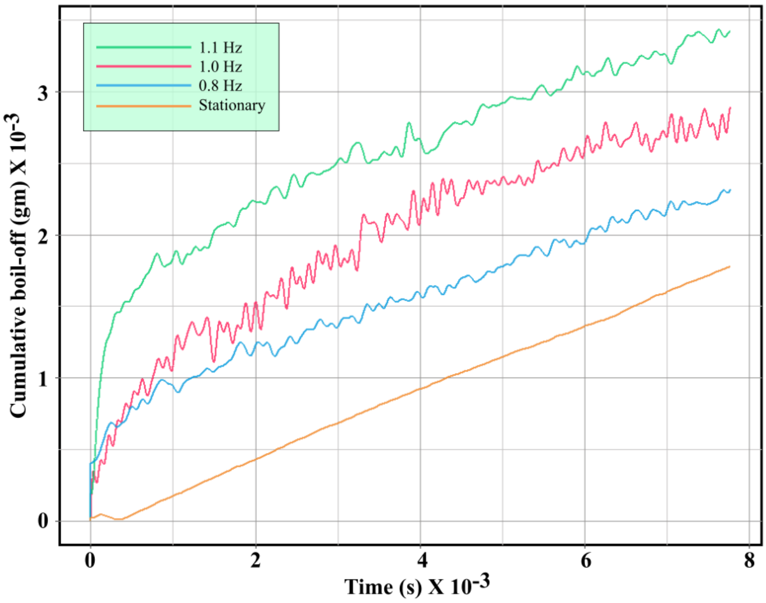

Figure 9: Mass reduction history for oscillations at different frequencies

The possible reasons for the enhanced boil-off are:

1. Conversion of the kinetic energy of the slosh wave hitting the wall into thermal energy when the liquid hits the tank walls [17]. Since this kinetic energy increases with an increase in the oscillation frequency [75], more thermal energy is generated at higher oscillation frequencies. Moreover, Rafiee et al. [76] reported that the amplitude of kinetic energy is maximum at the start of oscillation and decays thereafter. Thus the rate of liquid boil-off would vary not only with the oscillation frequency but also from the start of oscillation to a later time as the sloshing gets established at any oscillation frequency. Amount of thermal energy produced varies in these cases and dictates the energy available for the vaporization of the liquid cryogen. Hence, a sudden increase in the liquid boil-off was observed at the start of the experimental runs.
2. Increase in the interfacial area between the liquid and ullage vapor due to wave formation. Oscillation of the test vessel generates ripples at the liquid surface, thereby increasing the effective liquid-ullage interfacial area [66]. The ripples become more pronounced at higher oscillation frequencies, and hence cause an increase in the interfacial area. This leads to higher heat transfer between the liquid cryogen and the ullage vapor, and hence higher liquid boil-off.
3. Enhanced heat transfer from the ambient into the tank due to forced convection. It is known that the heat transfer rate from the surface of a cylinder at rest increases when an oscillatory motion is applied to the cylinder [77].

This is due to an increase in the heat transfer coefficient as forced convection ensues when the cylinder is in motion.

To explore the existence of the minimum oscillation frequency that would cause significant boil-off, due to sloshing, we compared the boil-off behaviour at different oscillation frequencies used in our study, at different time instants, as shown in Fig. 10.

The figure shows an almost linear variation of cumulative boil-off with frequency at all times. Therefore we performed a linear regression of the cumulative boil-off with the frequency at chosen time instants. The intersection of the regressed straight lines with the boil-off in stationary case indicated the existence of an incipient oscillation frequency (f_i in Fig. 10) that would be needed to induce significant boil-off due to sloshing. The incipient frequency increases as the time progresses. This signifies that the incipient frequency is more for lower liquid levels. This observation suggests that a given mass of a liquid cryogen should be transported in a shallow vessel with large lateral expanse rather than in tall vessels with smaller lateral expanse. Such an arrangement would defer significant sloshing induced boil-off.

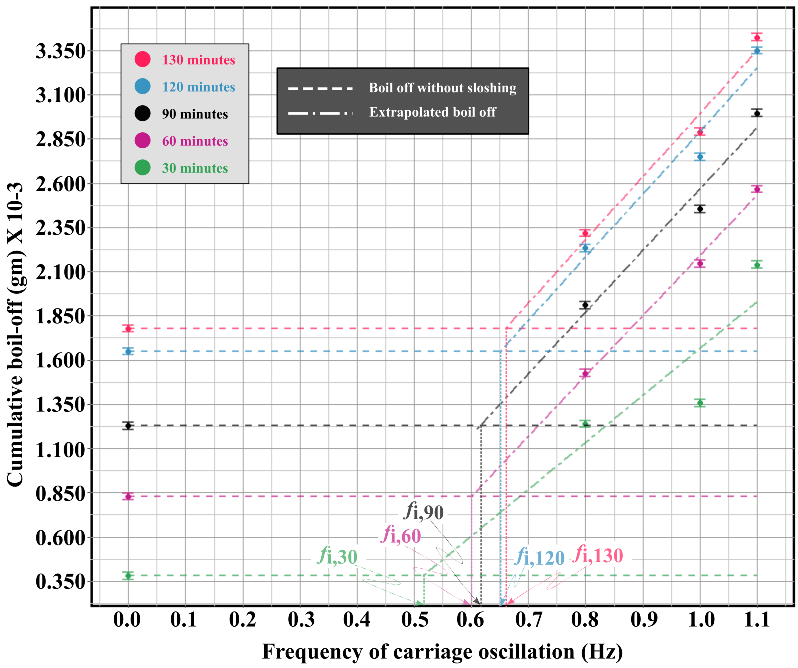

Figure 10: Cumulative boil-off vs frequency of oscillation at different time.

8. Conclusions

To the best of the authors knowledge, this study is the first to corroborate the earlier postulations on the enhanced boil-off due to liquid sloshing in mobile cryogenic storage tanks. This was achieved through the development of a first-of-its-kind experimental test facility capable of measuring the boil-off under different sloshing conditions. The salient conclusions from the study are :

1. The sloshing causes a significant increase in the boil-off; the enhancement could go as much as 90%.
2. The boil-off enhancement increases with an increase in the sloshing intensity
3. There exists an incipient frequency below which
    (a) The sloshing effect may be neglected in estimating the boil-off, and
    (b) The boil-off may be obtained by considering a stationary vessel.
4. The boil-off becomes more pronounced with an increase in the liquid fill level. Hence, the fill level should be kept at the minimum permissible while designing the storage system.

Future studies should be directed towards understanding the effect of shape and size of the vessel on the sloshing induced boil-off of cryogenic liquids.

9. Acknowledgements

The authors would like to acknowledge Mr. Sreekesh K, Dr. Ganesh Malayath, Ms. Gargi S Pillai and Dr. Jomy Joseph of Indian Institute of Technology Kharagpur for their valuable inputs on the development of the experimental setup. The experiments were conducted with the help of Mr. Rajendra Kumar, Mr. Samaresh Dey and Mr. Emel V Kurian of Process Intensification Laboratory, Cryogenic Engineering Centre, Indian Institute of Technology Kharagpur.

The authors like to specially thank Dr. Pritam Saha for his invaluable help in conducting the experiments and making of the manuscript.

References

[1] Smith JJ, Schneider G, Suslov D, Oschwald M, Haidn O. Steady-state high pressure lox/h2 rocket engine combustion. Aerospace Science and Technology 2007;11(1):39–47. doi:https://doi.org/10.1016/j.ast.2006.08.007.

[2] Yin L, Ju Y. Comparison and analysis of two processes for bog re-liquefaction in lng carrier with normal-temperature compressor. International Journal of Refrigeration 2020;115:9–17. doi:https://doi.org/10.1016/j.ijrefrig.2020.03.008.

[3] de Troya JJ, Alvarez C, Fernández-Garrido C, Carral L. Analysing the possibilities of using fuel cells in ships. International Journal of Hydrogen Energy 2016;41(4):2853–66. doi:https://doi.org/10.1016/j.ijhydene.2015.11.145.

[4] Mulot V, Benkhelifa H, Pathier D, Ndoye FT, Flick D. Measurement of food dehydration during freezing in mechanical and cryogenic freezing conditions. International Journal of Refrigeration 2019;103:329–38. doi:https://doi.org/10.1016/j.ijrefrig.2019.02.032.

[5] Love-Jones S, Magee P. Medical gases, their storage and delivery. Anaesthesia & intensive care medicine 2007;8(1):2–6. doi:https://doi.org/10.1053/j.mpaic.2006.10.006.

[6] Hugill J. High purity oxygen for steel making. The Canadian Journal of Chemical Engineering 1958;36(4):169–74. doi:https://doi.org/10.1002/cjce.5450360404.

[7] Brown T, McDonald J, Knight K, Hedayat A, Champion Jr R. Propellant management and conditioning within the x-34 main propulsion system. In: 34th AIAA/ASME/SAE/ASEE Joint Propulsion Conference and Exhibit. 1998, p. 3518. doi:https://doi.org/10.2514/6.1998-3518.

[8] Naruo Y, Tokudome SI, Ishii M, Higashino K. Design and operational aspect of lox/lh2 propulsion system of reusable vehicle testing (rvt). In: 10th AIAA/NAL-NASDA-ISAS International Space Planes and Hypersonic Systems and Technologies Conference. 2001, p. 1841. doi:https://doi.org/10.2514/6.2001-1841.

[9] Fesmire J, Johnson W. Cylindrical cryogenic calorimeter testing of six types of multilayer insulation systems. Cryogenics 2018;89:58–75. doi:https://doi.org/10.1016/j.cryogenics.2017.11.004.

[10] Taneda M, Ohtani T, Okuda M, Tsukuda J. Systematic analysis of characteristics for different types of multilayer insulations. In: Advances in Cryogenic Engineering. Springer; 1988, p. 305–11. doi:https://doi.org/10.1007/978-1-4613-9874-5_38.

[11] Caps R, Fricke J. Thermal conductivity of opacified powder filler materials for vacuum insulations 1. International Journal of Thermophysics 2000;21(2):445–52. doi:https://doi.org/10.1023/A:1006691731253.

[12] Hanzelka P, Dupák L, Krutil V, Krzyžánek V, Skoupỳ R, Srnka A, et al. Low conductive thermal insulation pad with high mechanical stiffness. International Journal of Refrigeration 2021;doi:https://doi.org/10.1016/j.ijrefrig.2021.09.019.

[13] Nitin B, Sandilya P, Chakraborty G. Optimal design of a helical coil support for dewars in fuel cell applications 2021;doi:https://doi.org/10.21203/rs.3.rs-770941/v1.

[14] Nitin B, Sandilya P. Structural and thermal analysis of dewar supports for low boil-off long duration storage of cryogenic liquids. Indian Journal of Cryogenics 2018;doi:https://doi.org/10.5958/2349-2120.2018.00005.5.

[15] Nitin B, Sandilya P, Chakraborty G. Design of dewar supports through topology optimization. In: IOP Conference Series: Materials Science and Engineering; vol. 755. IOP Publishing; 2020, p. 012054. doi:https://doi.org/10.1088/1757-899X/755/1/012054.

[16] Virdi PS, Nitin B, Sandilya P, Chakraborty G. Theoretical comparison of thermo-mechanical behavior of a tension rod and a coil as dewar support. Indian Journal of Cryogenics 2019;doi:https://doi.org/10.5958/2349-2120.2019.00038.4.

[17] Hands BA. Cryogenic Engineering. Academic Press Inc; 1986.

[18] Ibrahim RA. Liquid sloshing dynamics: theory and applications. Cambridge University Press; 2005. doi:https://doi.org/10.1017/CBO9780511536656.

[19] Faltinsen O, Timokha A. Sloshing 2017;.

[20] Abramson HN. The dynamic behavior of liquids in moving containers, with applications to space vehicle technology 1966;.

[21] Sun L, Kikuchi T, Goto Y, Hayashi M. Tuned liquid damper (tld) using heavy mud. WIT Transactions on The Built Environment 1998;38. doi:https://doi.org/10.2495/SM980081.

[22] Hoskins LM, Jacobsen LS. Water pressure in a tank caused by a simulated earthquake. Bulletin of the seismological society of America 1934;24(1):1–32. doi:https://doi.org/10.1785/BSSA0240010001.

[23] Ozeren Y, Wren D, Reba M. Wave-induced erosion of soil embankment in laboratory flume. Journal of Hydraulic Engineering

2021;147(4):04021011.

[24] Gurusamy S, Kumar D. Experimental study on nonlinear sloshing frequency in shallow water tanks under the effects of excitation amplitude and dispersion parameter. Ocean Engineering 2020;213:107761. doi:https://doi.org/10.1016/j.oceaneng.2020.107761.

[25] Rognebakke OF, Faltinsen OM. Coupling of sloshing and ship motions. Journal of Ship Research 2003;47(03):208–21.

[26] Lomen DO. Liquid propellant sloshing in mobile tanks of arbitrary shape. Tech. Rep.; 1965.

[27] Park YJ, Kim S, Cho JR, Doh DH, Cho GR. Fatigue life and effect of sloshing according to the scale ratio of a prismatic lng tank. Journal of Mechanical Science and Technology 2021;35(2):507–14. doi:https://doi.org/10.1007/s12206-021-0109-z.

[28] Ryan RS. A history of aerospace problems, their solutions, their lessons. National Aeronautics and Space Administration, Marshall Space Flight Center; 1996.

[29] Fujino Y, Pacheco BM, Chaiseri P, Sun LM. Parametric studies on tuned liquid damper (tld) using circular containers by free-oscillation experiments. Doboku Gakkai Ronbunshu 1988;1988(398):177–87.

[30] Bunnik T, Huijsmans R. Large scale lng sloshing model tests. In: The Seventeenth International Offshore and Polar Engineering Conference. OnePetro; 2007,.

[31] Panigrahy P, Saha U, Maity D. Experimental studies on sloshing behavior due to horizontal movement of liquids in baffled tanks. Ocean Engineering 2009;36(3-4):213–22. doi:https://doi.org/10.1016/j.oceaneng.2008.11.002.

[32] Pal N, Bhattacharyya S, Sinha P. Experimental investigation of slosh dynamics of liquid-filled containers. Experimental Mechanics 2001;41(1):63–9. doi:https://doi.org/10.1007/BF02323106.

[33] Nayak SK, Biswal KC. Fluid damping in rectangular tank fitted with various internal objects–an experimental investigation. Ocean Engineering 2015;108:552–62. doi:https://doi.org/10.1016/j.oceaneng.2015.08.042.

[34] Myrillas K, Planquart P, Buchlin JM, Schyns M. Small scale experiments of sloshing considering the seismic safety of myrrha. International Journal of Hydrogen Energy 2016;41(17):7239–51. doi:https://doi.org/10.1016/j.ijhydene.2016.01.158.

[35] Das SP, Hopfinger EJ. Parametrically forced gravity waves in a circular cylinder and finite-time singularity. Journal of Fluid Mechanics 2008;599:205–28. doi:https://doi.org/10.1017/S0022112008000165.

[36] Dodge FT, et al. The new" dynamic behavior of liquids in moving containers". Southwest Research Inst. San Antonio, TX; 2000.

[37] Popov G, Sankar S, Sankar T, Vatistas G. Liquid sloshing in rectangular road containers. Computers & fluids 1992;21(4):551–69. doi:https://doi.org/10.1016/0045-7930(92)90006-H.

[38] Warnitchai P, Pinkaew T. Modelling of liquid sloshing in rectangular tanks with flow-dampening devices. Engineering Structures 1998;20(7):593–600. doi:https://doi.org/10.1016/S0141-0296(97)00068-0.

[39] Dodge FT, Kana DD, Abramson HN. Liquid surface oscillations in longitudinally excited rigid cylindrical containers. Aiaa Journal 1965;3(4):685–95. doi:https://doi.org/10.2514/3.2948.

[40] Abramson HN, Chu WH, Garza LR. Liquid sloshing in spherical tanks. AIAA Journal 1963;1(2):384–9. doi:https://doi.org/10.2514/3.1542.

[41] Eswaran M, Reddy G. Liquid sloshing in fuel storage bays of advanced reactor subjected to earthquake loading. Procedia Engineering 2016;144:1278–85. doi:https://doi.org/10.1016/j.proeng.2016.05.118.

[42] Zhang Yx, Wan Dc, Takanori H. Comparative study of mps method and level-set method for sloshing flows. Journal of hydrodynamics, Ser B 2014;26(4):577–85. doi:https://doi.org/10.1016/S1001-6058(14)60065-2.

[43] Sanapala V, Velusamy K, Patnaik B. Cfd simulations on the dynamics of liquid sloshing and its control in a storage tank for spent fuel applications. Annals of Nuclear Energy 2016;94:494–509. doi:https://doi.org/10.1016/j.anucene.2016.04.018.

[44] Bryson AE. Control of spacecraft and aircraft; vol. 41. Princeton university press Princeton, New Jersey; 1993.

[45] Kang M, Kim J, You H, Chang D. Experimental investigation of thermal stratification in cryogenic tanks. Experimental Thermal and Fluid Science 2018;96:371–82. doi:https://doi.org/10.1016/j.expthermflusci.2017.12.017.

[46] de Quay L, Hodge BK. A history of collapse factor modeling and empirical data for cryogenic propellant tanks. In: 46th AIAA/ASME/SAE/ASEE Joint Propulsion Conference & Exhibit. 2010, p. 6559.

[47] Ludwig C, Dreyer M, Hopfinger E. Pressure variations in a cryogenic liquid storage tank subjected to periodic excitations. International Journal of Heat and Mass Transfer 2013;66:223–34. doi:https://doi.org/10.1016/j.ijheatmasstransfer.2013.06.072.

[48] Moran ME, McNelis NB, Kudlac MT, Haberbusch MS, Satornino GA. Experimental results of hydrogen slosh in a 62 cubic foot (1750 liter) tank. In: Joint Propulsion Conference. E-8916; 1994,.

[49] Konopka M, Noeding P, Klatte J, Behruzi P, Gerstmann J, Stark A, et al. Analysis of ln2 filling, draining, stratification and sloshing experiments. In: 46th AIAA fluid dynamics conference. 2016, p. 4272. doi:https://doi.org/10.2514/6.2016-4272.

[50] Kim GJ, Rhee H, Jeon WH, Jeong J, Hwang DS. Lateral sloshing analysis by cfd and experiment for a spherical tank. International Journal of Aeronautical and Space Sciences 2020;21(3):816–25. doi:https://doi.org/10.1007/s42405-020-00295-2.

[51] Snyder H. Effect of sloshing on the mechanics of dewar systems in low-gravity. Cryogenics 2001;41(11-12):825–32. doi:https://doi.org/10.1016/S0011-2275(01)00174-6.

[52] Liu Z, Feng Y, Lei G, Li Y. Hydrodynamic performance in a sloshing liquid oxygen tank under different initial liquid filling levels. Aerospace Science and Technology 2019;85:544–55. doi:https://doi.org/10.1016/j.ast.2019.01.005.

[53] Liu Z, Feng Y, Lei G, Li Y. Fluid sloshing dynamic performance in a liquid hydrogen tank. International Journal of Hydrogen Energy 2019;44(26):13885–94. doi:https://doi.org/10.1016/j.ijhydene.2019.04.014.

[54] Grotle EL, Æsøy V. Dynamic modelling of the thermal response enhanced by sloshing in marine lng fuel tanks. Applied Thermal Engineering 2018;135:512–20. doi:https://doi.org/10.1016/j.applthermaleng.2018.02.086.

[55] Xue MA, Lin P. Numerical study of ring baffle effects on reducing violent liquid sloshing. Computers & Fluids 2011;52:116–29. doi:https://doi.org/10.1016/j.compfluid.2011.09.006.

[56] Liu D, Lin P. A numerical study of three-dimensional liquid sloshing in tanks. Journal of Computational physics 2008;227(8):3921–39. doi:https://doi.org/10.1016/j.jcp.2007.12.006.

[57] Liu Z, Feng Y, Lei G, Li Y. Fluid thermal stratification in a non-isothermal liquid hydrogen tank under sloshing excitation. International Journal of Hydrogen Energy 2018;43(50):22622–35. doi:https://doi.org/10.1016/j.ijhydene.2018.10.113.

[58] Grotle EL, Halse KH, Pedersen E, Li Y, et al. Non-isothermal sloshing in marine liquefied natural gas fuel tanks. In: The 26th International Ocean and Polar Engineering Conference. OnePetro; 2016,.

[59] Agui JH, Moder JP. Modeling of non-isothermal cryogenic fluid sloshing. In: 51st AIAA/SAE/ASEE Joint Propulsion Conference. 2015, p. 4072. doi:https://doi.org/10.2514/6.2015-4072.

[60] Himeno T, Watanabe T, Nonaka S, Naruo Y, Inatani Y, Aoki H. Numerical and experimental investigation on sloshing in rocket tanks with damping devices. In: 43rd AIAA/ASME/SAE/ASEE joint propulsion conference & exhibit. 2007, p. 5557. doi:https://doi.org/10.2514/6.2007-5557.

[61] Liu Z, Feng Y, Lei G, Li Y. Sloshing hydrodynamic performance in cryogenic liquid oxygen tanks under different amplitudes. Applied Thermal Engineering 2019;150:359–71. doi:https://doi.org/10.1016/j.applthermaleng.2018.12.145.

[62] Loots E, Pastoor W, Buchner B, Tveitnes T. The numerical simulation of lng sloshing with an improved volume of fluid method. In: International Conference on Offshore Mechanics and Arctic Engineering; vol. 37432. 2004, p. 113–21. doi:https://doi.org/10.1115/OMAE2004-51085.

[63] Pistani F, Thiagarajan K. Experimental measurements and data analysis of the impact pressures in a sloshing experiment. Ocean engineering

2012;52:60–74. doi:https://doi.org/10.1016/j.oceaneng.2012.06.002.

[64] Arif UGM, Loo CY, Kang HS, Punurai W, Quen LK, Lai GNY, et al. Suppression of hydrodynamic sloshing in liquefied natural gas tank with floating baffle: Experimental and numerical studies. In: IOP Conference Series: Earth and Environmental Science; vol. 463. IOP Publishing; 2020, p. 012111. doi:https://doi.org/10.1088/1755-1315/463/1/012111.

[65] Grotle EL, Æsøy V. Numerical simulations of sloshing and the thermodynamic response due to mixing. Energies 2017;10(9):1338. doi:https://doi.org/10.3390/en10091338.

[66] Wu S, Ju Y. Numerical study of the boil-off gas (bog) generation characteristics in a type c independent liquefied natural gas (lng) tank under sloshing excitation. Energy 2021;223:120001. doi:https://doi.org/10.1016/j.energy.2021.120001.

[67] Jung JH, Yoon HS, Lee CY. Effect of natural frequency modes on sloshing phenomenon in a rectangular tank. International Journal of Naval Architecture and Ocean Engineering 2015;7(3):580–94. doi:https://doi.org/10.1515/ijnaoe-2015-0041.

[68] Housner GW. Dynamic pressures on accelerated fluid containers. Bulletin of the seismological society of America 1957;47(1):15–35. doi:https://doi.org/10.1785/BSSA0470010015.

[69] Krishnan R. Electric motor drives: modeling, analysis, and control. Pearson; 2001.

[70] Ghosh S, Nitin B, Remanan S, Bhattacharjee Y, Ghorai A, Dey T, et al. A multifunctional smart textile derived from merino wool/nylon polymer nanocomposites as next generation microwave absorber and soft touch sensor. ACS applied materials & interfaces 2020;12(15):17988–8001. doi:https://doi.org/10.1021/acsami.0c02566.

[71] Kelemençe İ, Yalçın ME. Dynamic weighing using a time-variant low pass filter. In: 2019 11th International Conference on Electrical and Electronics Engineering (ELECO). IEEE; 2019, p. 552–6. doi:https://doi.org/10.23919/ELECO47770.2019.8990494.

[72] Barron RF, Nellis GF. Cryogenic heat transfer. CRC press; 2017.

[73] Moffat RJ. Describing the uncertainties in experimental results. Experimental thermal and fluid science 1988;1(1):3–17.

[74] Ahn Y, Kim SY, Kim KH, Lee SW, Kim Y, Park JJ. Study on the effect of density ratio of liquid and gas in sloshing experiment. In: The Twenty-second International Offshore and Polar Engineering Conference. OnePetro; 2012,.

[75] Deng X, Tait M. Equivalent mechanical models of tuned liquid dampers with different tank geometries. Canadian Journal of Civil Engineering 2008;35(10):1088–101.

[76] Rafiee A, Pistani F, Thiagarajan K. Study of liquid sloshing: numerical and experimental approach. Computational Mechanics 2011;47(1):65–75. doi:https://doi.org/10.1007/s00466-010-0529-6.

[77] Fu WS, Tong BH. Numerical investigation of heat transfer from a heated oscillating cylinder in a cross flow. International Journal of Heat and Mass Transfer 2002;45(14):3033–43.